

MICROCOPY RESOLUTION TEST CHART
NBS 1010A

54

LEVEL II

12

ADA 087281

THRUSTING CHARACTERISTICS OF PROPULSORS

W. S. Gearhart and E. P. Bruce

DTIC
SELECTED
JUL 29 1980
C D

Technical Memorandum
File No. TM 80-118
30 May 1980
Contract No. N00024-79-C-6043

Copy No. 18

The Pennsylvania State University
APPLIED RESEARCH LABORATORY
Post Office Box 30
State College, PA 16801

NAVY DEPARTMENT

NAVAL SEA SYSTEMS COMMAND

Approved for Public Release
Distribution Unlimited

DOC FILE COPY

80 7 28 138

14 ARL/FSU/TM 20-118

UNCLASSIFIED

SECURITY CLASSIFICATION OF THIS PAGE (When Data Entered)

REPORT DOCUMENTATION PAGE		READ INSTRUCTIONS BEFORE COMPLETING FORM
1. REPORT NUMBER TM 80-118	2. GOVT ACCESSION NO. AD-A087281	3. RECIPIENT'S CATALOG NUMBER
4. TITLE (and Subtitle) THRUSTING CHARACTERISTICS OF PROPULSORS	5. TYPE OF REPORT & PERIOD COVERED Technical Memorandum	
7. AUTHOR(s) W. S. Gearhart and E. P. Bruce	6. PERFORMING ORG. REPORT NUMBER	
9. PERFORMING ORGANIZATION NAME AND ADDRESS Applied Research Laboratory Post Office Box 30 State College, PA 16801	8. CONTRACT OR GRANT NUMBER(s) N00024-79-C-6043	
11. CONTROLLING OFFICE NAME AND ADDRESS Naval Sea Systems Command Washington, DC 20362	10. PROGRAM ELEMENT, PROJECT, TASK AREA & WORK UNIT NUMBERS 14-3	
14. MONITORING AGENCY NAME & ADDRESS (if different from Controlling Office)	12. REPORT DATE 30 May 1980	
	13. NUMBER OF PAGES 27	
	15. SECURITY CLASS. (of this report) UNCLASSIFIED	
	15a. DECLASSIFICATION/DOWNGRADING SCHEDULE	
16. DISTRIBUTION STATEMENT (of this Report) Approved for Public Release. Distribution Unlimited. Per NAVSEA - 27 June 1980.		
17. DISTRIBUTION STATEMENT (of the abstract entered in Block 20, if different from Report)		
18. SUPPLEMENTARY NOTES		
19. KEY WORDS (Continue on reverse side if necessary and identify by block number) propulsors, thrust, loss, slipstream		
20. ABSTRACT (Continue on reverse side if necessary and identify by block number) The function of any propulsive system, is to provide a forward thrust along its axis. The design objective is to obtain a maximum in propulsor thrust with a minimum of shaft power while satisfying practical limits of propulsor size, shaft speed, and cavitation resistance. The generation of thrust requires that some kinetic energy be lost in the propulsive slipstream. These losses are associated with both axial and rotational velocity components in the slipstream. In addition, the presence of rotational velocity in the slipstream results in a		

DD FORM 1473 1 JAN 73

EDITION OF 1 NOV 65 IS OBSOLETE

UNCLASSIFIED

SECURITY CLASSIFICATION OF THIS PAGE (When Data Entered)

391007

J.R.

UNCLASSIFIED

SECURITY CLASSIFICATION OF THIS PAGE (When Data Entered)

20. low pressure region in the far wake which reduces the net effective thrust generated by the propulsor. It has been the tradition of the propulsor designer to neglect the rotational effects, other than considering the kinetic energy losses, since it is assumed that the rotational component of velocity in the far wake is small. This assumption is valid for propulsors that ingest large mass flows and place a small amount of energy per unit mass in the flow. However, the trend now is toward more heavily loaded propulsors, both of the open or ducted type. Thus, a reevaluation of the relative magnitudes of the losses associated with the velocity components in the propulsive slipstream is necessary.

It is the intent of this paper to evaluate, for a given shaft power, the relative losses in propulsor thrust associated with the axial and rotational velocity components in the slipstream. The magnitude of each of these effects is a function of propulsor advance ratio, ingested mass flow, energy per unit mass imparted to the flow, and the ratio of the radius of the inner core to the radius of the slipstream in the far wake. The radial loading distribution, for significant rotation in the slipstream, differs considerably from that normally assumed as optimum for cases where slipstream rotation is ignored. The thrust per unit power developed by propulsors of various types as a function of the above operating parameters is derived assuming an inviscid fluid. The results provide the designer with a means to determine the penalties associated with rotation in the far wake, and the gains that can be achieved by removing the rotation.

Accession For	
NTIS GRA&I	<input checked="" type="checkbox"/>
DDC TAB	<input type="checkbox"/>
Unannounced	<input type="checkbox"/>
Justification	
By _____	
Distribution/ _____	
Availability _____	
Dist	Avail and/or special
<input checked="" type="checkbox"/>	<input type="checkbox"/>

UNCLASSIFIED

SECURITY CLASSIFICATION OF THIS PAGE (When Data Entered)

Subject: Thrusting Characteristics of Propulsors

References: See page 27.

Abstract: The function of any propulsive system, is to provide a forward thrust along its axis. The design objective is to obtain a maximum in propulsor thrust with a minimum of shaft power while satisfying practical limits of propulsor size, shaft speed, and cavitation resistance. The generation of thrust requires that some kinetic energy be lost in the propulsive slipstream. These losses are associated with both axial and rotational velocity components in the slipstream. In addition, the presence of rotational velocity in the slipstream results in a low pressure region in the far wake which reduces the net effective thrust generated by the propulsor. It has been the tradition of the propulsor designer to neglect the rotational effects, other than considering the kinetic energy losses, since it is assumed that the rotational component of velocity in the far wake is small. This assumption is valid for propulsors that ingest large mass flows and place a small amount of energy per unit mass in the flow. However, the trend now is toward more heavily loaded propulsors, both of the open or ducted type. Thus, a reevaluation of the relative magnitudes of the losses associated with the velocity components in the propulsive slipstream is necessary.

It is the intent of this paper to evaluate, for a given shaft power, the relative losses in propulsor thrust associated with the axial and rotational velocity components in the slipstream. The magnitude of each of these effects is a function of propulsor advance ratio, ingested mass flow, energy per unit mass imparted to the flow, and the ratio of the radius of the inner core to the radius of the slipstream in the far wake. The radial loading distribution, for significant rotation in the slipstream, differs considerably from that normally assumed as optimum for cases where slipstream rotation is ignored. The thrust per unit power developed by propulsors of

30 May 1980
WSG:EPB:cag

various types as a function of the above operating parameters is derived assuming an inviscid fluid. The results provide the designer with a means to determine the penalties associated with rotation in the far wake, and the gains that can be achieved by removing the rotation.

Acknowledgements: This work was sponsored by NAVSEA. Special thanks are given to R. F. Davis, who programmed this procedure and provided the data for the illustrations.

Nomenclature

A_B	reference area
Q	mass flow rate
V_θ	tangential velocity imparted to fluid at rotor tip
V_j	velocity in jet
ΔV	change in axial velocity of slipstream
V_i	velocity of inflow to propulsor
U	tangential velocity of rotor
V_∞	velocity of ship
V_θ	tangential velocity of fluid
r_j	radius of downstream jet
r_B	reference radius
r_i	radius of upstream jet
r_t	radius of rotor tip
r_h	radius of rotor hub
R	radius of cylindrical control volume
F_x	axial force generated by the propulsor
p_∞	freestream or ambient static pressure
p_c	static pressure on surface of inner core
p_j	static pressure in jet
C_m	mass-flow-rate coefficient
C_x	axial-force coefficient
ψ	head coefficient $\left(2 \frac{U V_0}{V_\infty V_\infty} \right)$
T	axial thrust
H	head placed in fluid
J	advance ratio $\left(\frac{V_\infty}{n 2r_B} \right)$

n shaft speed (rps)
K constant
k ratio of inner core radius to jet radius
 η_p propulsive coefficient
 C_p shaft power coefficient $\left(\frac{\text{Rotor Power}}{\rho/2 V_\infty^3 A_B} = \psi C_m \right)$
 γ fluid density

Introduction

The literature has defined propulsive efficiency as the ratio of the net thrust generated by the propulsor times the forward speed of the propulsor divided by the shaft power required [1]*.

This ratio, which has been termed the propulsive coefficient, can attain values greater than unity if the inflow velocity relative to the propulsor is substantially less than the forward speed of the propulsor [2].

The present analysis will consider only an ideal efficiency, i.e., an inviscid fluid is assumed, frictional losses on any blading or ducting associated with the propulsor are neglected. On this basis, and within the assumptions stated for the cases considered, the propulsive coefficients obtained are the highest that can be expected. Naturally, the inclusion of real fluid effects will lead to lower values than are indicated herein.

Van Lammeran, et al, [3] recognized the effects of tangential velocities in the slipstream and the resulting reduction in the net thrust of the propulsor due to low pressure in the slipstream. Durand [1], who also derived relationships that considered these effects, concluded that the complexity introduced in the solution to the equations for evaluating both the kinetic-energy and pressure-drag terms was not warranted for propulsors being considered (lightly loaded).

It is the intent of this study to derive the relationships necessary to evaluate the effects of tangential velocities both inside and outside the inner core to a propulsor slipstream. In so doing, the improved performance achieved by eliminating the swirl will become apparent for heavily loaded propulsors ingesting small mass flows and rotating with low relative velocities. This will provide the designer with a means of determining when these effects should be considered and their relative magnitudes. The results also indicate that when the effects of slipstream swirl are included, the radial distribution of blade loading has a strong influence on the net thrust and efficiency of the propulsor.

Rotor-Stator System; No Swirl in Slipstream

The first configuration considered is a rotor-stator system designed in a manner such that no tangential velocity (V_0) exists downstream of the propulsor (i.e., at Station 2 in Figure 1). In addition, referring to Figure 1, the following are assumed:

- (a) The pressure acting on the surfaces of the control volume is p_∞ .
- (b) The dimensions, $R \gg r_i$; $R \gg r_j$; $R \gg r_t$; $r_t \gg r_h$.

*Numbers in brackets designate references listed on page 27.

- (c) The tangential velocity imparted to the fluid by the rotor provides radially constant angular momentum, i.e. spanwise circulation is constant.

The relationships developed are sufficiently general to consider an inflow velocity, relative to the propulsor, that differs from the forward speed of the propulsor. The average velocity out of the downstream face of the control volume due to the jet velocity will, in most cases, be greater than the average inflow velocity at the upstream face. From continuity, there must be a mass flow through the sides of the cylinder. It is assumed that this inflow of fluid to the control volume is in the axial direction (i.e. it contains a very small radial component which may be neglected). This mass flow, Q , is given by

$$\begin{aligned} Q &= \rho(\pi r_j^2) V_j + \rho[\pi(R^2 - r_j^2)] V_\infty - \rho(\pi r_i^2) V_i \\ &\quad - \rho[\pi(R^2 - r_i^2)] V_\infty \\ &= \rho\pi[(r_j^2 V_j - r_i^2 V_i) - V_\infty(r_j^2 - r_i^2)] \end{aligned} \quad (1)$$

The force required to hold the propulsor stationary is given by the momentum theorem as

$$\begin{aligned} F_x &= [\rho(\pi r_j^2) V_j] V_j + [\rho\pi(R^2 - r_j^2) V_\infty] V_\infty - [\rho(\pi r_i^2) V_i] V_i \\ &\quad - [\rho\pi(R^2 - r_i^2) V_\infty] V_\infty - [\rho\pi(r_j^2 V_j - r_i^2 V_i) - \rho\pi V_\infty(r_j^2 - r_i^2)] V_\infty \\ &= \rho\pi \left[r_j^2 V_j^2 - r_i^2 V_i^2 - (r_j^2 V_j - r_i^2 V_i) V_\infty \right] \end{aligned} \quad (2)$$

The energy equation written for a streamline through the propulsor (Station 1 to Station 2) with $V_j = V_i + \Delta V$ is

$$p_\infty + 1/2 \rho V_i^2 = p_\infty + 1/2 \rho (V_i + \Delta V)^2 - \rho U V_\theta \quad ,$$

where U represents the rotor tangential velocity.

This expression if divided by $\rho V_\infty^2/2$ can be nondimensionalized and written as

$$\left(\frac{\Delta V}{V_\infty}\right)^2 + 2\left(\frac{V_i}{V_\infty}\right) \left(\frac{\Delta V}{V_\infty}\right) - 2\left(\frac{U}{V_\infty}\right) \left(\frac{V_\theta}{V_\infty}\right) = 0 \quad .$$

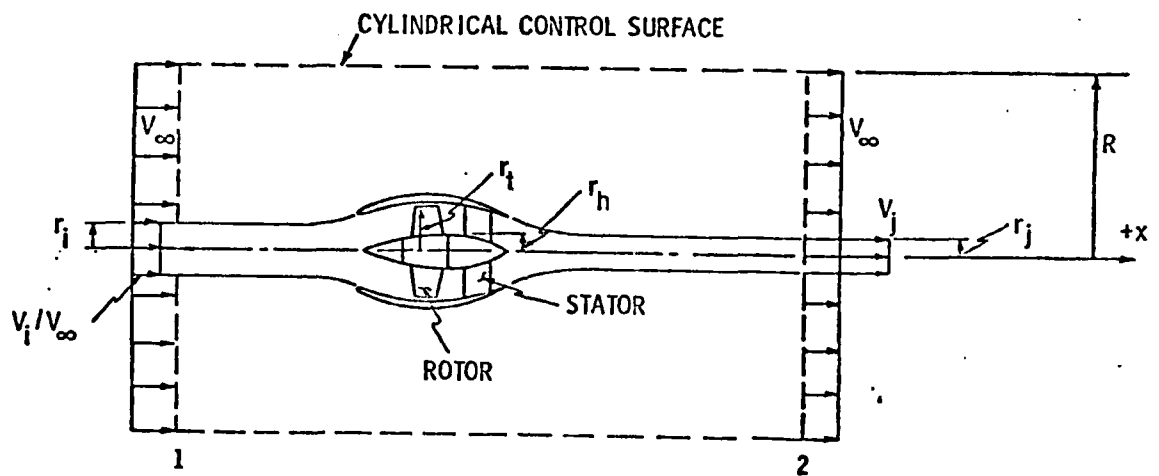


Figure 1 - Control Volume for No Swirl in Slipstream

The solution to this quadratic equation defines the change in axial velocity between Stations 1 and 2 as

$$\left(\frac{\Delta V}{V_\infty}\right) = -\left(\frac{V_i}{V_\infty}\right) + \sqrt{\left(\frac{V_i}{V_\infty}\right)^2 + 2\left(\frac{U}{V_\infty}\right)\left(\frac{V_\theta}{V_\infty}\right)} \quad (3)$$

The jet velocity, $V_j = V_i + \Delta V$, is constant across the jet since the quantity $2\left(\frac{U}{V_\infty}\right)\left(\frac{V_\theta}{V_\infty}\right)$ is constant. Thus, it follows that

$$\frac{V_j}{V_\infty} = \sqrt{\left(\frac{V_i}{V_\infty}\right)^2 + 2\left(\frac{U}{V_\infty}\right)\left(\frac{V_\theta}{V_\infty}\right)} \quad (4)$$

The continuity equation permits the following relation to be written between Station 1 and 2:

$$\rho(\pi r_i^2) V_i = \rho(\pi r_j^2) V_j \quad .$$

A mass flow rate coefficient can be defined as

$$C_m = \frac{\rho(\pi r_i^2) V_i}{\rho(\pi r_B^2) V_\infty} = \left(\frac{r_i}{r_B}\right)^2 \left(\frac{V_i}{V_\infty}\right) = \left(\frac{r_i}{r_B}\right)^2 \left(\frac{V_j}{V_\infty}\right) \quad (5)$$

where r_B is some selected reference dimension.

The force generated by the propulsor, presented in coefficient form, is

$$C_x = \frac{F_x}{1/2 \rho V_\infty^2 \pi r_B^2} \quad (6)$$

The relations given by (2) and (5) can be substituted in (6) to obtain

$$C_x = 2 \left(\frac{V_i}{V_\infty}\right) \left(\frac{r_i}{r_B}\right)^2 \left(\frac{V_j - V_i}{V_\infty}\right) \quad (7)$$

This relation indicates that, for a propulsor with no swirl in the slipstream, the thrust generated is directly proportional to the mass flow rate and the change in axial velocity imparted to the fluid between Stations 1 and 2. Equation (7) can be rewritten, using Equation (4) and

the head coefficient $\psi = 2 \frac{U V_\theta}{V_\infty V_\infty}$, as

$$C_x = 2 C_m \left\{ -\frac{V_i}{V_\infty} + \left(\frac{V_i}{V_\infty} \right)^2 + \psi \right\}. \quad (8)$$

The work per unit time generated by the propulsor is the product $(F_x)(V_\infty)$ which, in nondimensional terms, is equivalent to C_x . The shaft power is the energy per unit time placed in the fluid, assuming no frictional losses and, in nondimensional terms, is the product of the mass flow rate coefficient C_m and the head coefficient ψ . The propulsive coefficient is the ratio

$$\eta_p = \frac{F_x V_\infty}{\text{Shaft Power}} = \frac{C_x}{\psi C_m} = \frac{2}{\psi} \left\{ -\frac{V_i}{V_\infty} + \sqrt{\left(\frac{V_i}{V_\infty} \right)^2 + \psi} \right\}. \quad (9)$$

The preceding relations permit an evaluation of the force characteristics and the relative efficiency of a propulsor with no swirl in the slipstream as a function of the head coefficient, mass-flow-rate coefficient, and inlet velocity ratio.

If a case is considered where $V_i/V_\infty = 1.0$, the selection of a particular head coefficient immediately specifies the jet velocity ratio from Equation (4). Considering a given mass flow rate coefficient, the ratio of slipstream radii can be obtained from Equation (5). If a duct is located along some portion of the slipstream as shown in Figure 2a, it is obvious that the net thrust and efficiency obtained are completely independent of rotor and stator location in the duct or slipstream. In similar fashion, the shape of the duct has no influence on these characteristics, and a propulsor with a shroud configuration as shown in Figure 2b would produce the same thrust and have the same efficiency as that of Figure 2a. This assumes that the same head and mass flow rate coefficients are associated with the propulsor in both cases. The minimum pressure on the blade would be significantly affected by the rotor location and by the shape of the duct. The ratio of shaft thrust to duct thrust dictates the shape of the duct, the rotor and stator location and the advance ratio. However, assuming an inviscid flow, the net thrust coefficient and the efficiency are independent of these parameters for given head and mass flow rate coefficients. This is also true for an unducted rotor-stator system designed for zero swirl in the downstream jet.

Shown in Figure 3 is a plot of the power ratio, or propulsive coefficient, as a function of head coefficient for propulsive devices that have no swirl in the downstream jet. These results apply for any mass flow rate coefficient or advance ratio.

This figure indicates that, for inflow velocity ratios less than unity, propulsive coefficients greater than unity can be achieved. A discussion of this characteristic was presented in Reference [2] and proceeds as follows. The propulsive coefficient is defined as

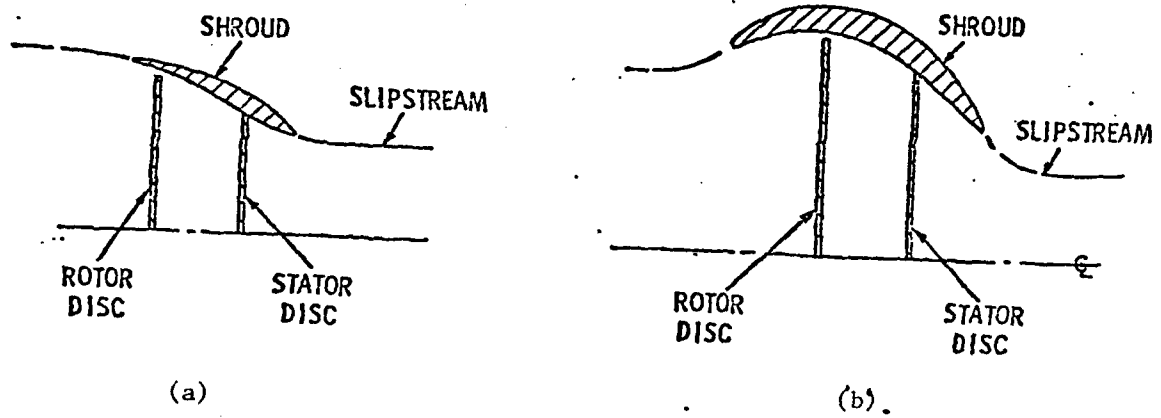


Figure 2 - Ducted Propulsor Configurations of Equal Performance

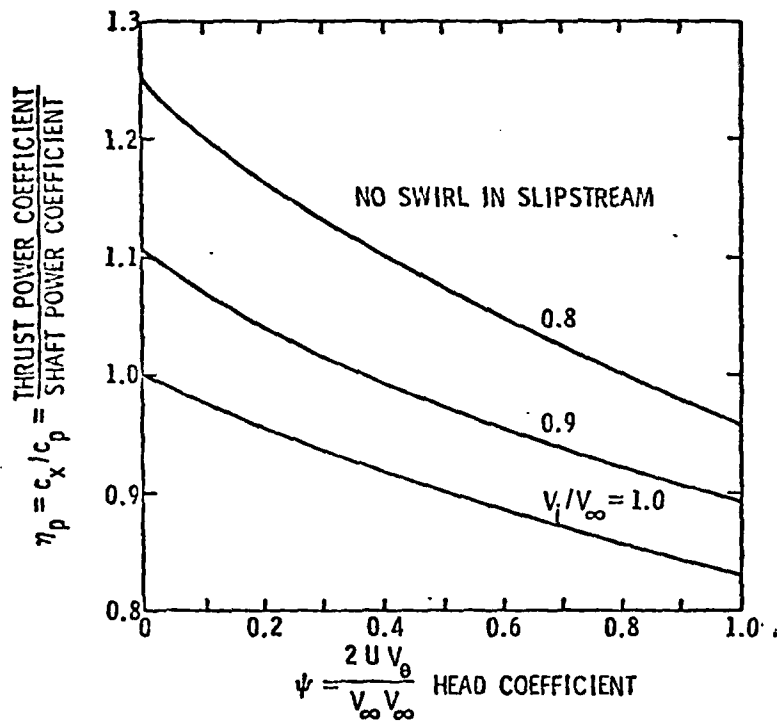


Figure 3 - Propulsive Coefficient as a Function of an Inflow Velocity Ratio

$$\eta_p = \frac{\text{Thrust Power}}{\text{Shaft Power}} = \frac{F_x V_\infty}{H Q \gamma} = \frac{(\rho Q \Delta V) (V_\infty)}{H Q \gamma}$$

The energy equation previously written between Stations 1 and 2 can be expressed as

$$\rho U V_\theta = \gamma H = \frac{1}{2} \rho (2V_i \Delta V + \Delta V^2)$$

Then the propulsive coefficient becomes

$$\eta_p = \frac{(\rho Q \Delta V) (V_\infty)}{(\rho Q \Delta V) (V_i + \frac{\Delta V}{2})} = \frac{1}{\frac{V_i}{V_\infty} + \frac{1}{2} \frac{\Delta V}{V_\infty}}$$

For a given mass flow rate, it is apparent that the thrust developed is proportional to $(\frac{\Delta V}{V})$. It is also evident that ingesting fluid at an inflow velocity (V_i/V_∞) of reduced magnitude reduces the power required to produce this thrust and, therefore, increases the propulsive coefficient.

Rotor System; Swirl in Slipstream

An open or ducted propulsor with no stator system results in a slipstream having a rotational component of velocity. This rotational velocity reduces the net thrust produced by the propulsor in two ways. First, a portion of the shaft energy is lost due to the kinetic energy associated with the rotational velocity. In addition, the rotation in the slipstream creates a low-pressure region that results in a reduction of the net thrust generated at a given level of shaft power. In the following paragraphs, relationships are developed that define the net thrust produced by a propulsor with swirl in the slipstream. They are based on Figure 4 and the following assumptions:

- (a) The pressure acting on the surface of the control volume is p_∞ everywhere except in the exit jet of radius r_j .
- (b) The pressure in the exit jet is a function of radius and must be equal to p_∞ immediately inside the boundary of the jet.
- (c) The dimensions $R \gg r_i$, $R \gg r_j$, $R \gg r_t$ and $r_t \gg r_h$.
- (d) The tangential velocity V_θ is not equal to zero in the downstream jet.
- (e) The V_θ distribution in the downstream jet consists of a free vortex distribution in the outer core and a solid body rotational inner core whose effect on the axial velocity may be neglected.

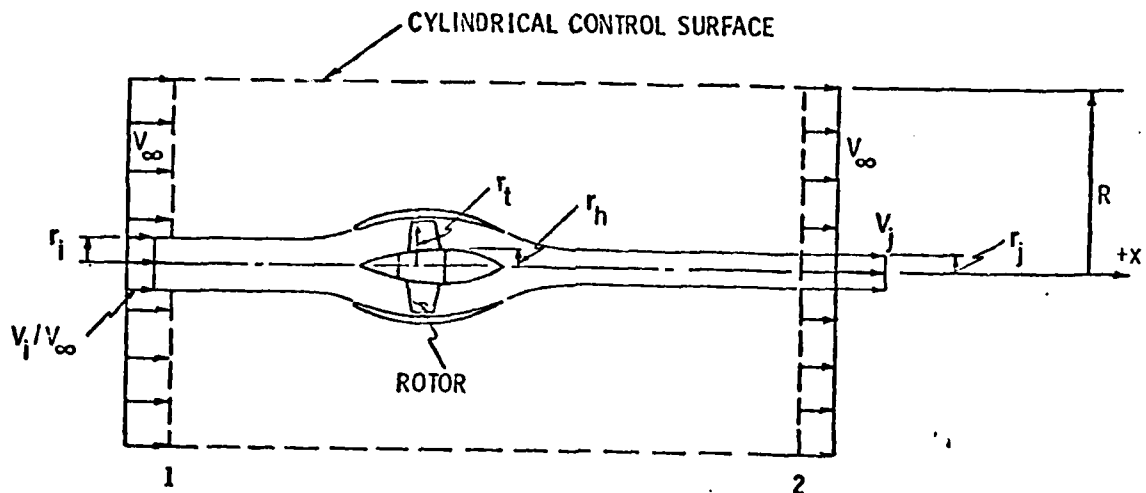


Figure 4 - Control Volume for Swirl in Slipstream

To satisfy continuity (as shown in the previous section) there may be a mass flow through the sides of the cylinder. This mass flow, Q, is given by

$$Q = \rho\pi (r_j^2 V_j - r_i^2 V_i) - \rho\pi V_\infty (r_j^2 - r_i^2) \quad . \quad (10)$$

Applying the momentum theorem to the control volume leads to the expression

$$\begin{aligned} p_\infty(\pi R^2) - p_\infty[\pi(R^2 - r_j^2)] - 2\pi \int_0^j p_j r dr + F_x &= [\rho(\pi r_j^2) V_j] V_j + \\ [\rho\pi(R^2 - r_j^2) V_\infty] V_\infty - [\rho(\pi r_i^2) V_i] V_i - [\rho\pi(R^2 - r_i^2) V_\infty] V_\infty - \\ [\rho\pi(r_j^2 V_j - r_i^2 V_i) - \rho\pi V_\infty(r_j^2 - r_i^2)] V_\infty \quad , \end{aligned}$$

which may be solved for the force F_x required to hold the propulsor stationary. Thus,

$$F_x = \rho\pi \left[r_j^2 V_j^2 - r_i^2 V_i^2 - (r_j^2 V_j - r_i^2 V_i) V_\infty \right] + 2\pi \int_0^j (p_j - p_\infty) r dr \quad . \quad (11)$$

The energy equation for a streamline through the propulsor (Station 1 to Station 2) with $V_j = V_i + \Delta V$ is

$$p_\infty + \frac{1}{2} \rho V_i^2 = p_j + \frac{1}{2} \rho [(V_i + \Delta V)^2 + V_\theta^2] - \rho U V_\theta \quad ,$$

which can be written in nondimensional form as

$$\left(\frac{\Delta V}{V_\infty}\right)^2 + 2 \frac{V_i}{V_\infty} \frac{\Delta V}{V_\infty} + \left[\left(\frac{V_\theta}{V_\infty}\right)^2 - 2 \left(\frac{U}{V_\infty}\right) \left(\frac{V_\theta}{V_\infty}\right) + \frac{p_\infty - p_j}{1/2 \rho V_\infty^2} \right] = 0$$

The solution to this equation is

$$\frac{\Delta V}{V_\infty} = -\frac{V_i}{V_\infty} + \sqrt{\left(\frac{V_i}{V_\infty}\right)^2 + 2 \left(\frac{U}{V_\infty}\right) \left(\frac{V_\theta}{V_\infty}\right) - \left(\frac{V_\theta}{V_\infty}\right)^2 + \frac{p_\infty - p_j}{1/2 \rho V_\infty^2}} \quad . \quad (12)$$

The velocity of the jet, V_j , is given by $V_j = V_i + \Delta V$; therefore,

$$\frac{V_j}{V_\infty} = \sqrt{\left(\frac{V_i}{V_\infty}\right)^2 + 2 \left(\frac{U}{V_\infty}\right) \left(\frac{V_\theta}{V_\infty}\right) - \left(\frac{V_\theta}{V_\infty}\right)^2 + \frac{p_\infty - p_j}{1/2\rho V_\infty^2}} \quad (13)$$

It will be shown later that the quantity $\left[- \left(\frac{V_\theta}{V_\infty}\right)^2 + \frac{p_\infty - p_j}{1/2\rho V_\infty^2} \right]$ is a constant

and, therefore, the jet velocity is a constant for the conditions considered. As in the previous section, the continuity equation relates the mass flow rate to the upstream and downstream slipstream conditions and leads to the expression

$$C_m = \left(\frac{r_i}{r_B}\right)^2 \left(\frac{V_i}{V_\infty}\right) = \left(\frac{r_j}{r_B}\right)^2 \left(\frac{V_j}{V_\infty}\right) \quad (14)$$

The force coefficient C_x is again defined as in Equation (6) and by use of Equations (11) and (14), the expression for C_x may be written as

$$C_x = 2 \left(\frac{V_i}{V_\infty}\right) \left(\frac{r_i}{r_B}\right)^2 \left(\frac{V_j - V_i}{V_\infty}\right) + 4 \int_0^{r_j} \frac{(p_j - p_\infty) r dr}{\rho V_\infty^2 r_B^2} \quad (15)$$

The last term in the above equation is the pressure drag resulting from the rotation in the slipstream. The term is negative, as shown below, since p_∞ is greater than the pressure in the jet, p_j ; thus, it reduces the net thrust of the propulsor. This term can be evaluated by considering a free vortex with $V_\theta r = \text{constant} = K$ in the outer core region and a solid-body rotation with $V_\theta = k_1 r$ in a small inner core near the axis. The pressure in the jet, p_j , in the outer core region where the free vortex distribution exists can be expressed as

$$\frac{1}{\rho} \frac{\partial p_j}{\partial r} = \frac{V_\theta^2}{r} = \frac{K^2}{r^3}$$

Integrating this relation from any radius r to the jet radius r_j (where p_∞ exists) leads to the relation

$$p_j - p_\infty = \rho \frac{K^2}{2} \left[\frac{1}{r_j^2} - \frac{1}{r^2} \right] \quad (16)$$

If the maximum radius r_c of the inner core is given by $r_c = k r_j$, then the pressure on the surface of the inner core, p_c , is given by

$$p_c - p_\infty = \rho \frac{K^2}{2} \left[\frac{1}{r_j^2} - \frac{1}{k^2 r_j^2} \right] = \rho \frac{K^2}{2 r_j^2} \left[\frac{k^2 - 1}{k^2} \right] \quad (17)$$

Inside the inner core, $V_\theta = k_1 r$ and, at the boundary that separates the two core regions, $k_1 r_c = \frac{K}{r_c}$; therefore, $k_1 = \frac{K}{k^2} \left(\frac{1}{r_j^2} \right)$. Thus, by the radial equilibrium equation, the difference in pressure between the inner-core outer radius r_c and any inner-core radial position is

$$p_c - p_j = \rho \frac{k_1^2}{2} (r_c^2 - r^2)$$

On the inner core outer radius, $r_c = kr_j$, and

$$p_c - p_j = \rho \frac{k_1}{2} (r^2 - k^2 r_j^2) \quad (18)$$

Adding Equations (18) and (19) defines the pressure in the inner core, where solid body rotation exists, as

$$p_j - p_\infty = \rho \frac{K^2}{2 k^4 r_j^4} \left[r^2 - k^2 r_j^2 (2 - k^2) \right] \quad (19)$$

The integral in Equation (15) can now be evaluated. In the outer region of the jet where free vortex rotation exists:

$$\begin{aligned} \int_{kr_j}^{r_j} (p_j - p_\infty) r dr &= \rho \frac{K^2}{2} \int_{kr_j}^{r_j} \left(\frac{1}{r_j^2} - \frac{1}{r^2} \right) r dr \\ &= \rho \frac{K^2}{4} \left[1 - k^2 - 2 \ln \left(\frac{1}{k} \right) \right] \quad (20) \end{aligned}$$

In the inner core region of the jet, the following applies:

$$\begin{aligned} \int_0^{kr_j} (p_j - p_\infty) r dr &= \rho \frac{K^2}{2 k^4 r_j^4} \int_0^{kr_j} [r^2 - k^2 r_j^2 (2 - k^2)] r dr \\ &= \rho \frac{K^2}{8} (2k^2 - 3) \quad (21) \end{aligned}$$

Substituting Equations (13), (20) and (21) into Equation (15), and noting

that $C_m = \left(\frac{r_i}{r_B}\right)^2 \left(\frac{v_i}{v_\infty}\right)$, leads to the expression

$$C_x = 2 C_m \left[-\frac{v_i}{v_\infty} + \sqrt{\left(\frac{v_i}{v_\infty}\right)^2 + \psi - \left(\frac{v_\theta}{v_\infty}\right)^2 \left(\frac{r_t}{r_B}\right)^2} \right] + \left(\frac{v_\theta}{v_\infty}\right)^2 \left(\frac{r_t}{r_B}\right)^2 \left[1 - k^2 - 2 \ln \left(\frac{1}{k}\right) \right] + \frac{1}{2} \left(\frac{v_\theta}{v_\infty}\right)^2 \left(\frac{r_t}{r_B}\right)^2 (2k^2 - 3) \quad (22)$$

If Equation (22) is compared with Equation (8), it is apparent that additional terms are present. The next to last term in Equation (22) is the force increment associated with the low pressure in the outer region of the rotational jet, and the last term is the force increment associated with the inner core of the jet. The last term under the radical sign is the kinetic energy loss associated with the rotational velocity in the jet, and it also reduces the net thrust of the propulsor. The efficiency of propulsion, as defined by Equation (9), can be expressed as

$$\eta_p = \frac{2}{\psi} \left\{ \left[-\frac{v_i}{v_\infty} + \sqrt{\left(\frac{v_i}{v_\infty}\right)^2 + \psi - \left(\frac{v_\theta}{v_\infty}\right)^2 \left(\frac{r_t}{r_B}\right)^2} \right] + \frac{1}{2C_m} \left(\frac{v_\theta}{v_\infty}\right)^2 \left(\frac{r_t}{r_B}\right)^2 \left[1 - k^2 - 2 \ln \left(\frac{1}{k}\right) \right] + \frac{1}{4C_m} \left(\frac{v_\theta}{v_\infty}\right)^2 \left(\frac{r_t}{r_B}\right)^2 (2k^2 - 3) \right\} \quad (23)$$

It is apparent, from a comparison of Equations (9) and (23), that the efficiency of a propulsor that leaves swirl in the exit jet is a function of many more parameters than is the efficiency of a propulsor with no swirl in the exit flow. The additional parameters can be identified more clearly if it is noted that

$$\left(\frac{v_\theta}{v_\infty}\right)^2 \left(\frac{r_t}{r_B}\right)^2 = \frac{\left(\frac{J}{\pi}\right)^2 \left(\frac{\psi}{2}\right)^2 \left(\frac{v_i}{v_\infty}\right)}{C_m}$$

$$\left(\frac{v_\theta}{v_\infty}\right)^2 \left(\frac{r_t}{r_B}\right)^2 = \left(\frac{J}{\pi}\right)^2 \left(\frac{\psi}{2}\right)^2$$

$$\text{and } k = \frac{r_c}{r_j}$$

In contrast to the propulsor with zero swirl in the jet, it is obvious that while holding all other parameters constant, η_p decreases as advance ratio increases. It is also evident that the efficiency will increase if all other parameters are held constant and the mass-flow-rate coefficient C_m is increased. Because the ratio of inner core radius to jet radius, k , has a strong influence on efficiency, as the ratio $\frac{r_c}{r_j}$ decreases, the efficiency decreases.

It should be emphasized that for a given shaft power, mass flow rate, advance ratio, inlet velocity ratio, and core radius ratio, the ratio of the slipstream jet diameter and upstream diameter is established. Consider a ducted propulsor designed to provide the energy input associated with a given slipstream contraction. The point to be emphasized here is that the rotor could be located anywhere along the axis of an arbitrarily shaped duct provided that the proper tangential turning at the rotor tip is specified. Thus, the thrust generated and the propulsive coefficient are both independent of either duct shape or rotor location. This is true since angular momentum is preserved (i.e. $V_\theta r = K$) and the energy per unit mass, or head, $\frac{U V_\theta}{g}$ that is imparted to each fluid particle is constant and is not

dependent on rotor location. Therefore, for the same advance ratio, if the rotor is located in the slipstream where its tip diameter is large, then U is large, and V_θ is small. Conversely, if the rotor is located in a smaller cross-section of the slipstream, the rotor speed U is small but V_θ must be large. Figure 5 shows four individual propulsor configurations. The configurations have different shrouds and rotor locations but have the same mass flow rate, advance ratio, inlet velocity ratio, and shaft power. The net thrust and propulsive coefficient of all four of these units would be equal if the ratio r/r_j and the circulation at the blade tip is equal in all cases. However, rotor blade loading, and the ratio of shaft thrust to shroud thrust would be different in each case.

The problem that must be solved, employing the equations derived for the case of a slipstream with rotation, is that of determining the net thrust and propulsive coefficient generated as a function of mass flow rate, head coefficient, inlet velocity ratio, advance ratio, and assumed ratio of core-to-jet radius. This has been done by employing an iteration procedure to solve the appropriate equations. The energy equation, (13), defines the following relationship for the jet velocity:

$$v_j/v_\infty = \sqrt{\left(\frac{v_i}{v_\infty}\right)^2 + \psi - \left(\frac{v_{\theta t}}{v_\infty}\right)^2 \left(\frac{r_t}{r_j}\right)^2} \quad (24)$$

This expression can be combined with the continuity equation to produce the relation

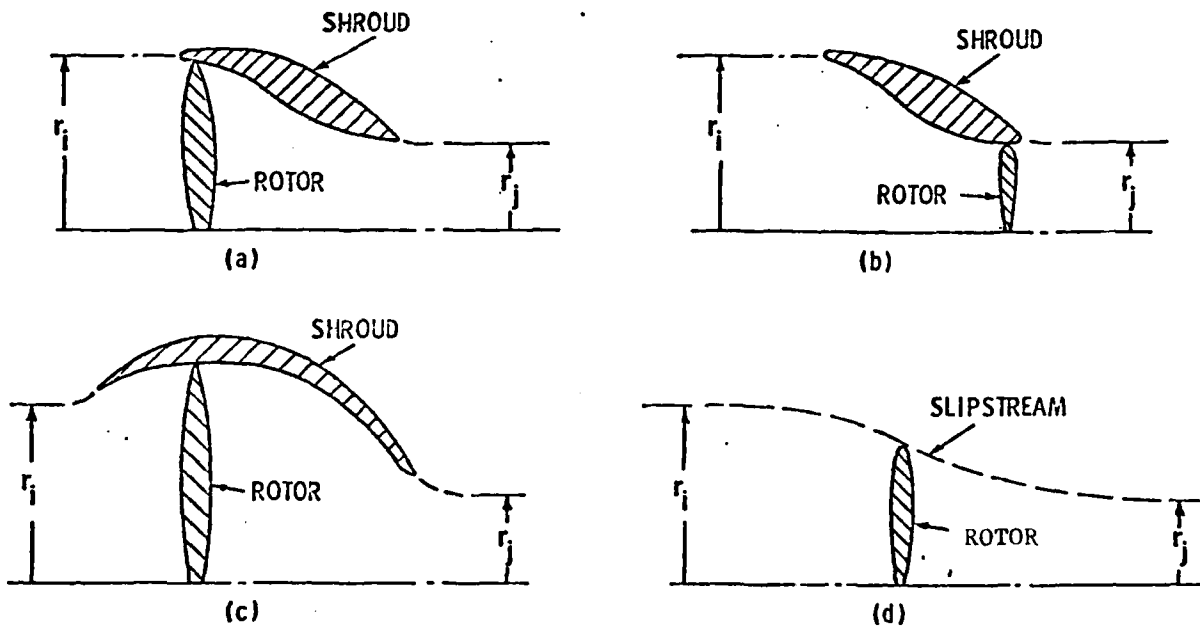


Figure 5 - Propulsor Configurations of Equal Performance with Swirl in Slipstream

$$\left(\frac{r_j}{r_B}\right)^4 = \frac{C_m^2}{\left(\frac{V_j}{V_\infty}\right)^2} = \frac{C_m^2}{\left(\frac{V_j}{V_\infty}\right)^2 + \psi - \left(\frac{V_\theta}{V_\infty}\right)^2 \left(\frac{r_t}{r_j}\right)^2}$$

and, since

$$\left(\frac{V_\theta}{V_\infty}\right)^2 \left(\frac{r_t}{r_j}\right)^2 = \left(\frac{\psi}{2}\right)^2 \left(\frac{J}{\pi}\right)^2 \frac{V_j/V_\infty}{C_m}$$

the jet radius can be expressed as

$$r_j/r_B = \left[\frac{C_m^2}{\left(\frac{V_j}{V_\infty}\right)^2 + \psi - \frac{\left(\frac{\psi}{2}\right)^2 \left(\frac{J}{\pi}\right)^2 \frac{V_j}{V_\infty}}{C_m} \right]^{1/4} \quad (25)$$

For specified values of C_m , V_j/V_∞ , ψ , and J , the iterative procedure is initiated by assuming a value of the ratio r_t/r_j and solving Equation (24). The value of V_j/V_∞ obtained is then substituted in Equation (25), and the ratio r_j/r_B is computed. This value of r_j/r_B is employed in computing r_t/r_j from the relation

$$\frac{r_t/r_B}{r_j/r_B} = \frac{J(U/V_\infty)}{r_j/r_B} \quad (26)$$

A solution is obtained when the equality shown in Equation (24) is satisfied.

Discussion of Results

A graphical presentation of the individual terms in Equation (22) is shown in Figure 6a for the case where the input parameters are as listed on the figure. It is apparent the drag increments due to swirl in the slipstream are considerably greater than those associated with the tangential kinetic energy losses in the slipstream. If one moves along a constant ψ -line, the shaft power coefficient is a constant. It is evident

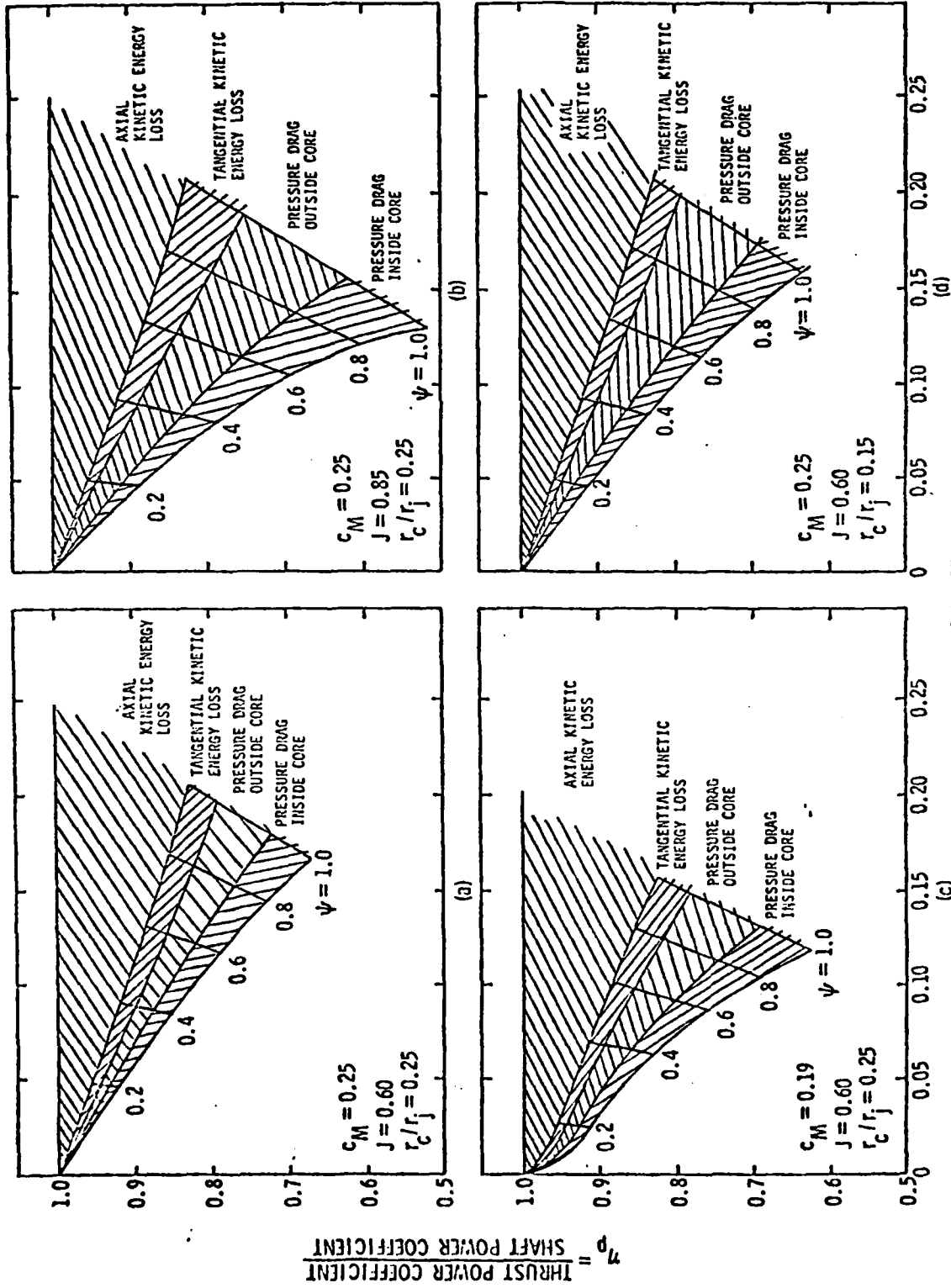


Figure 6 - Propulsor Performance as a Function of Various Parameters ($\frac{V_1}{V_\infty} = 1.0$)

that considerably gains in propulsor thrust and propulsive coefficient can be achieved by the use of a means that would eliminate or reduce the swirl in the slipstream.

The effect of increasing advance ratio but maintaining all else constant is shown in Figure 6b. The thrust and efficiency would remain the same as that in Figure 6a if no swirl existed in the slipstream. However, with swirl the losses at the higher advance ratio are significantly increased for the same shaft power coefficient.

A comparison of Figures 6a and 6c illustrated the effect of changing mass flow rate through the propulsor while maintaining all else constant. It is apparent that to achieve the same thrust coefficient with a lower mass flow coefficient, the propulsive coefficient will be reduced. This will require a higher shaft power coefficient and results from an increase in all components of the losses, as indicated by the Figures 6a and 6b. These two figures again indicate the advantage of eliminating swirl in the slipstream. For the reduced-flow-rate propulsor, the same net thrust could be achieved with a smaller propulsor at a higher efficiency if swirl were removed from the slipstream. Considering a required thrust coefficient of unity, the propulsive coefficient obtained at a mass flow rate $C_m = 0.190$, is 0.91 with no swirl in the slipstream. At a mass flow rate $C_m = 0.250$, the propulsive coefficient is 0.71 when swirl exists in the slipstream.

In similar fashion a comparison of Figure 6a and 6b indicates that the same thrust coefficient can be achieved at a higher advance ratio with a higher efficiency if swirl is eliminated from the slipstream. In this instance (from Figure 6b), with a thrust coefficient of unity and $C_m = 0.25$, the propulsive coefficient at an advance ratio of 0.85 and zero swirl is 0.91. From Figure 6a with $C_m = 0.25$ and $C_x = 1.0$ at an advance ratio of 0.60, the propulsive coefficient obtained is 0.83 with swirl in the slipstream.

The preceding illustrates that the pressure drag caused by swirl in the slipstream is a significant contribution to the performance of a propulsor. This effect has been neglected in the past under the assumption that the tangential kinetic energy placed in the flow was small. For lightly loaded propulsors this assumption can be made with little error in performance predictions but it must be considered for moderately or heavily loaded propulsors.

An assumption that strongly influences the magnitude of the pressure drag contribution is the ratio of inner core radius to jet radius. This ratio cannot be computed but can be estimated based on a survey of several experimental traverses taken downstream of various propellers. Traverse data obtained using a laser doppler velocimeter is presented in [4]. The data in Reference [4] indicated the ratio to be about 0.15, however, the use of r_c/r_j of 0.25, is considered a more conservative limit for this parameter and is, therefore, recommended. The relative effect on the predicted performance is obtained by comparing Figures 6a and 6d. The smaller r_c/r_j ratio results in about an additional 3-4 percent lower propulsive coefficient at this mass flow rate and advance ratio. At

smaller mass flow rates and higher advance ratios, this increment of loss becomes significantly greater for r_c/r_j less than 0.25.

The preceding exercise showing the effects of $\frac{r_c}{r_j}$ illustrates, for propulsors with swirl in the slipstream, that the efficiency and thrust of the unit can be improved by reducing the loading near the root and increasing the loading near the midspan and tip. This differs from the classical definition of optimum spanwise loading to provide a minimum in loss of energy. According to the Rankine-Froude theory [1], the thrust should be uniformly distributed over the whole propeller disc.

The significance of an inflow velocity ratio V_i/V_∞ that is less than unity and its effect on the propulsive coefficient has been discussed. An illustration of the difference in thrust coefficient and propulsive coefficient that can be achieved by ingesting fluid having an inflow velocity ratio less than unity is shown by comparing Figures 6a and 7. By ingesting an inflow with $V_i/V_\infty = 0.90$, an increase of about 12% in propulsive coefficient can be obtained at a C_x of unity. Thus, a significant effect on efficiency results from ingesting fluid with a velocity in the upstream slipstream that is less than free stream. A reduced inflow velocity could result by ingesting boundary layer fluid.

Reasonably good agreement between experimental and analytical predictions of powering performance have been reported in Reference [6] for propulsors that have swirl in the slipstream. The prediction technique has neglected the effects of the pressure drag in the far wake which have been shown to contribute substantially to the propulsor efficiency. If the effects of both the reduced inflow and the pressure drag has been neglected, they would tend to cancel, and this would explain the good agreement. A second possibility exists because certain configurations have the rudder located immediately downstream of the propulsor in the slipstream. The presence of the control appendage would tend to reduce the swirl outside the inner core and reduce this drag increment. The inner core is probably not affected much, since it deflects and passes around the control appendage in a relatively stable core. On this basis, the contribution of the inner core to the drag would still remain and should be considered. In the flow outside the inner core the reduction of the swirl by the control appendage is an inefficient process and would result in relatively high energy losses. A far more effective means would be the use of vanes either forward or aft of the rotor as discussed in Reference [7].

Model powering predictions include corrections for parameters such as thrust deduction factors and hull efficiency which are largely based on empirical data. These corrections tend to compensate for neglecting the pressure drag due to swirl. However, to be properly applied, these corrections must account for changes in pressure drag as a function of the variables described.

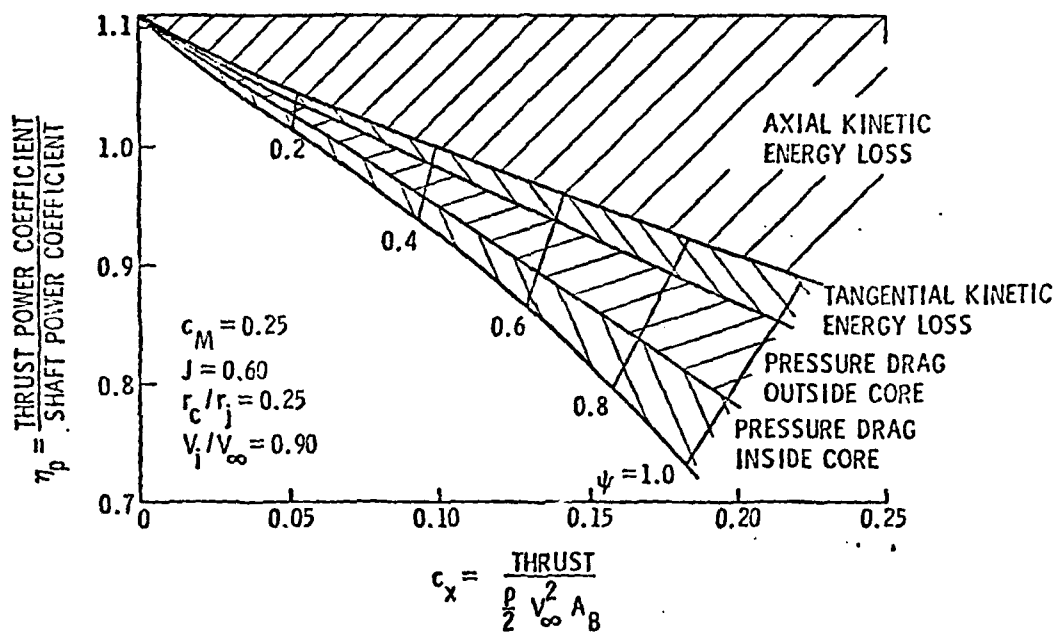


Figure 7 - Performance with Reduced Inflow Velocity

A large quantity of model powering data has been reported that used downstream drive systems. These data should be used with caution, since the pressure-drag terms would be operating on the surfaces of the shaft housing, and dynamometer and the total propulsor thrust measurements would be in error.

The effects of the pressure drag acting over the face of the downstream slipstream were experimentally demonstrated in Reference [8] where a backup bar, supported by a separate strut, was located downstream of a propulsor. This bar was faired-in with the contour of the propulsor hub just downstream of the propulsor exit. At the design advance ratio, with the backup bar in place, the shaft thrust was increased by 17 percent.

Figure 8 shows efficiencies and thrust coefficients as a function of advance ratio for propulsors ingesting mass flow rates of 0.16, 0.20, and 0.25. For the same efficiency, the figure indicates that higher thrust coefficients can be obtained over the advance ratio range if swirl is removed from the slipstream. The gains in thrust coefficient become greater as advance ratio increases. These figures also illustrate that by eliminating swirl, a smaller propulsor (i.e. lower mass flow rate) can be designed that will have the same efficiency and thrust as would be obtained with a large propulsor that had swirl in the slipstream.

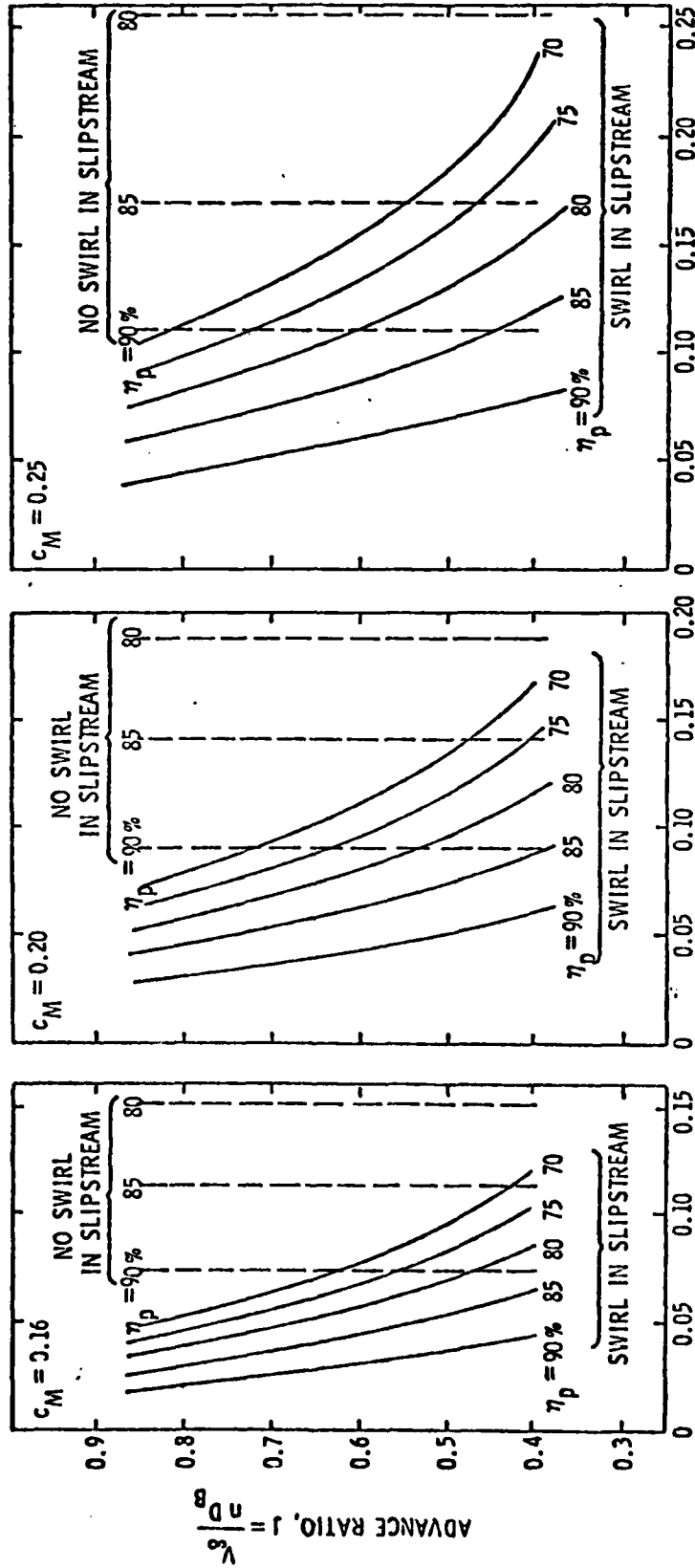
The possibility to design for smaller diameter rotors with the same efficiency and thrust is illustrated by Figure 8 if it is considered that the rotor tip diameter is approximately proportional to the square root of the mass flow coefficient. Therefore, the tip diameter of a rotor ingesting a mass flow of 0.16 is about 0.8 that of a rotor ingesting a mass flow of 0.25. If a thrust coefficient of 0.10 and a propulsive coefficient of no less than 80% is required, then a maximum advance ratio of 0.65 at a C_m of 0.25 can be obtained with a propulsor with swirl in the slipstream. However, by eliminating swirl, these conditions could be achieved at a C_m of 0.16 over the entire advance ratio range plotted at an efficiency of about 87%.

Summary and Conclusions

The preceding analysis indicates that the pressure drag that originates from swirl in the slipstream is of significant magnitude and must be considered in the design and performance predictions of moderately or heavily loaded propulsors.

The magnitude of the pressure drag increment is strongly dependent on advance ratio and mass flow rate of the propulsor. The pressure drag is also dependent on the radial spanwise loading distribution.

The propulsive coefficient and total propulsor thrust are reduced by swirl in the slipstream by two means: the kinetic energy loss associated with the tangential velocity of the slipstream and the drag due to the reduced pressure across the slipstream jet. The latter contribution is greater for the cases analyzed than the kinetic energy losses.



$$c_x = \frac{\text{THRUST}}{\rho \frac{V_\infty^2}{2} A_B}$$

Figure 8 - Propulsor Performance with Varying Mass Flow Rates $\left(\frac{V_1}{V_\infty} = 1.0; \frac{r_c}{r_j} = 0.25 \right)$

For certain ranges of advance ratio and mass flow rates, (i.e. rotor diameter) significant gains in efficiency and propulsor thrust can be obtained for a given shaft horsepower if swirl is removed from the slipstream.

The total thrust and efficiency of a ducted propulsor with swirl in the slipstream and operating with given values of advance ratio, inflow velocity ratio, r_c/r_j , mass flow, and head coefficient are independent of shroud shape or location of the rotor in the shroud.

Propulsor powering data obtained using a dynamometer mounted downstream of the propulsor could be in error, because the pressure forces, due to swirl, do not operate over the propulsor disk as they do in the actual application.

References

- [1] Durand, W. F., Aerodynamic Theory, Volume IV, Dover Publications, Inc., New York, 1963.
- [2] Wislicenus, G. F., "Hydrodynamic and Propulsion of Submerged Bodies," J. Am. Rocket Soc., Vol. 30, 1960, pp. 1140-1148.
- [3] Van Lammeran, W. P. A., Troost, L., Koning, J. C., Resistance, Propulsion and Steering of Ships, Vol. II, The Technical Publishing Company, H. Stam - Haarlem - Holland, 1948.
- [4] Billet, M. L., "Mean Flow Measurements Near the Plane of an Open Rotor Operating with an Inlet Velocity Gradient," Joint Fluid Engr. Gas Turbine Conference, New Orleans, LA, March 10 - 13, 1980.
- [5] Billet, M. L., "Secondary Flow Generated Vortex Cavitation," Twelfth Symposium on Nava' Hydrodynamics; Washington, DC, June 1978.
- [6] Van Manen, J. D., and Oosterveld, M. W. C., "Analysis of Ducted Propellers Design," Society of Naval Architects and Marine Engineers, Annual Meeting, Paper No. 13, 1966.
- [7] Gearhart, W. S. and Henderson, R. E., "Performance of a Ducted Propeller Fitted to Surface Craft," Proceedings of the Eighteenth Meeting of the American Towing Tank Conference, Volume I, August 1977, Annapolis, Maryland.
- [8] McCormick, B. W. (et. al.), "A Study of Torpedo Propellers - Part I," Ordnance Research Laboratory, Report #16597-5, March 1956.

DISTRIBUTION LIST FOR ARL UNCLASSIFIED TM 80-118 by W. S. Gearhart and E. P. Bruce
dated 30 May 1980

Commander
Naval Sea Systems Command
Department of the Navy
Washington, DC 20362
Attn: Library
Code NSEA 09G32
(Copies No. 1 and 2)

Naval Sea Systems Command
Attn: Code NSEA 0342
(Copies No. 3 and 4)

Naval Sea Systems Command
Attn: T. E. Peirce
Code NSEA 63R3
(Copy No. 5)

Naval Sea Systems Command
Attn: A. R. Paladino
Code NSEA 05H1
(Copy No. 6)

Naval Sea Systems Command
Attn: F. Peterson
Code NSEA 52P
(Copy No. 7)

Defense Technical Information Center
5010 Duke Street
Cameron Station
Alexandria, VA 22314
(Copies No. 8 through 19)

Commanding Officer
Naval Underwater Systems Center
Newport, RI 02840
Attn: Library
Code 54
(Copy No. 20)

Commanding Officer
Naval Ocean Systems Center
San Diego, CA 92152
Attn: D. Nelson
Code 6342
(Copy No. 21)

Naval Ocean Systems Center
Attn: M. Reischman
Code 2542
(Copy No. 22)

Naval Ocean Systems Center
Attn: Library
(Copy No. 23)

Commanding Officer & Director
David W. Taylor Naval Ship R&D Center
Department of the Navy
Bethesda, MD 20084
Attn: W. B. Morgan
Code 15
(Copy No. 24)

David W. Taylor Naval Ship R&D Center
Attn: R. Cumming
Code 1544
(Copy No. 25)

David W. Taylor Naval Ship R&D Center
Attn: J. McCarthy
Code 154
(Copy No. 26)

David W. Taylor Naval Ship R&D Center
Attn: M. Sevik
Code 19
(Copy No. 27)

David W. Taylor Naval Ship R&D Center
Attn: W. K. Blake
Code 1905
(Copy No. 28)

Commanding Officer & Director
David W. Taylor Naval Ship R&D Center
Department of the Navy
Annapolis Laboratory
Annapolis, MD 21402
Attn: J. G. Stricker
Code 2721
(Copy No. 29)

Commander
Naval Surface Weapon Center
Silver Spring, MD 20910
Attn: Library
(Copy No. 30)

Naval Postgraduate School
Department of Aeronautics, Code 57
Monterey, CA 93940
Attn: Dr. Allen E. Fuhs
(Copy No. 31)

DISTRIBUTION LIST FOR ARL UNCLASSIFIED TM 80-118 by W. S. Gearhart and E. P. Bruce
dated 30 May 1980

Office of Naval Research Branch Office
1030 East Green Street
Pasadena, CA 91106
Attn: Dr. Rudolph J. Marcus
(Copy No. 32)

Office of Naval Research Branch Office
435 South Clark Street
Chicago, IL 60605
Attn: Commander
(Copy No. 33)

Office of Naval Research Branch Office
495 Summer Street
Boston, MA 02210
Attn: Commander
(Copy No. 34)

Office of Naval Research
Power Branch
Department of the Navy
Arlington, VA 22217
Attn: Mr. J. R. Patton
(Copy No. 35)

Office of Naval Research
Fluid Dynamics Branch, Code 438
Department of the Navy
Washington, DC 22217
Attn: Mr. Morton Cooper
(Copy No. 36)

Naval Ship Research and Development Center
Annapolis Division
Annapolis, MD 21402
Attn: Library
Code A214
(Copy No. 37)

University of Salford
Salford, M5 4WT
England
Attn: Dr. John H. Horlock
Vice Chancellor
(Copy No. 38)

Netherlands Ship Model Basin
P.O. Box 28
6700 AA Wageningen
The Netherlands
Attn: Dr. P. van Oossanen
(Copy No. 39)

Admiralty Marine Technology Establishment
Teddington, Middlesex
England
Attn: Dr. Allen Moore
(Copy No. 40)

Von-Karman Institute for Fluid Dynamics
Turbomachinery Laboratory
Rhode-Saint-Genese
Belgium
Attn: Library
(Copy No. 41)

NASA Lewis Research Center
21000 Brookpark Road
Cleveland, OH 44135
Attn: M. J. Hartman
MS 5-9
(Copy No. 42)

Commander
David W. Taylor Naval Ship R&D Center
Department of the Navy
Bethesda, MD 20084
Attn: R. J. Boswell
(Copy No. 43)

Massachusetts Institute of Technology
77 Massachusetts Avenue
Cambridge, MA 02139
Attn: J. Kerwin
(Copy No. 44)

P. Leehey
Massachusetts Institute of Technology
77 Massachusetts Avenue
Cambridge, MA 02139
(Copy No. 45)

J. Breslin
Stevens Institute of Technology
Davidson Laboratory
Castle Point Station
Hoboken, NJ 07030
(Copy No. 46)

Dr. Bruce D. Cox
7900 Inverness Ridge Road
Potomac, MD 20854
(Copy No. 47)

DISTRIBUTION LIST FOR ARL UNCLASSIFIED TM 80-118 by W. S. Gearhart and E. P. Bruce
dated 30 May 1980

Dr. G. F. Wislicenus
351 Golf Court (Oakmont)
Santa Rosa, CA 95405
(Copy No. 48)

Applied Research Laboratory
The Pennsylvania State University
P.O. Box 30
State College, PA 16801
Attn: R. E. Henderson
(Copy No. 49)

Applied Research Laboratory
Attn: W. S. Gearhart
(Copy No. 50)

Applied Research Laboratory
Attn: GTWT Files
(Copy No. 51)

HRB Singer Inc.
Science Park Road
State College, PA 16801
Attn: E. P. Bruce
(Copy No. 52)

ATE
LMED
-8